Biomaterials and Polymers Horizon (2022) 1(1)
https://doi.org/10.37819/bph.001.02.0136

RESEARCH ARTICLE

# Bio-based castor oil and lignin sulphonate: aqueous dispersions and shape-memory films

**Samy A. Madbouly**[1,2]

[1]*Behrend College, School of Engineering, Pennsylvania State University, Erie, Pennsylvania 16563, United States. Email: sum1541@psu.edu*
[2]*Department of Chemistry, Faculty of Science, Cairo University, Giza 12613, Egypt .*



## ABSTRACT

Aqueous polyurethane dispersions based on castor oil and lignin sulphonate (LS) were successfully synthesized in homogenous solution with nanoscale PU-lignin particle sizes as small as 35 nm. The particles size was found to be LS independent, while the dispersion viscosity increases dramatically with increasing the LS content. The increase in viscosity with increasing LS content was explained based on the chemical structure of LS. The LS is a water-soluble material and chemically reacted with diisocyanate to become a part of the dispersion particle (i.e., the nanoparticles is in fact a mixture or copolymer of castor oil-based polyurethane and lignin dispersed in water). The affinity of the PU-LS nanoparticle towards water could be increased with increasing the content of LS. Therefore, the PU-LS nanoparticle can adsorb thick water layer with increasing the LS content. According to this suggestion, the free water in the dispersion would significantly decrease and consequently the dispersion viscosity increases considerably. The cross-link density was also increase with increasing the LS content of the thin films obtained from dispersion cast. The PU-LS thin films obtained from dispersion cast showed an excellent shape-memory effect and the shape recovery was found to be strongly LS dependent. Furthermore, the supper critical $CO_2$ solution was used successfully to create three-dimensional porous structure of PU-LS with cell size depends on LS content. The temporary folded shape of PU-LS with 5 wt.% LS changed to its permanent shape (plane stripe) within just 17 s once the sample was immersed in a water bath at the programing temperature.

**ARTICLE HISTORY**
Received: 12-08-2021
Revised: 24-10-2021
Accepted: 25-11-2021

**KEYWORDS**
Polyurethane
Aqueous dispersions
Lignin
Rheology
Shape-memory
TEM

## Introduction

Most plastic materials commonly used in different industries, such as packaging, automotive, biomedical, oil and gas, etc. are produced entirely from petroleum-based products with only few exception (Mishra *et al*., 2022, Araby *et al*., 2021, Ionescu, 2021, Hussain *et al*. 2022, Yan, *et al*., 2022). The high crude oil prices as well as environmental concerns related to petroleum-based products have triggered a search for feedstocks and biorenewable materials including thermoplastic elastomer, such as polyurethane. Great attention has been devoted to establishing sustainability and green chemistry to replacing petroleum-based polymers with more environmentally friendly biopolymers from renewable resources (Jiménez *et al*., 2016, Zafar

*et al*., 2016, Wróblewska-Krepsztul *et al*., 2018, Zhao *et al*., 2018, Kumar *et al*., 2022, Dahy *et al*., 2017, Jamróz *et al*., 2019, Visakh *et al*., 2019, El-Sherbiny *et al*., 2017, Gutiérrez *et al*., 2017, Mowafi *et al*. 2018, Shi *et al*., 2016, Mittal *et al*., 2022). It is very crucial to develop inexpensive, renewable, natural materials as alternatives to petroleum-based products that will have a significant positive impact on the polymer industry and the environment. Plant oils are renewable materials used widely to obtain new green or sustainable monomers to synthesis large number of new bio-based polymers with outstanding mechanical, thermal, and biodegradable properties with similar performance to that of petroleum-based polymers and composites (Xia *et al*., 2010, Kundu *et al*., 2005, Andjelkovic *et al*. 2006, Yuan *et al*., 2015, Gandini *et al*., 2016, Zhu *et al*., 2016, Wu *et al*., 2018). The different triglyceride fatty acids of plant oils can be chemically modified with large number of reactive groups, such as hydroxyl, amine, carboxylic acid, epoxy, etc. to polymerize or copolymerize new bio-based polymers with outstanding multifunctional properties. All plant oils with the exception of castor oil, need chemical modification to obtain polyols for synthesis of PUs. The four most common routes to prepare plant oil-based polyols are: (1) epoxidation/oxirane ring opening; (2) transesterification/amidation; (3) hydroformylation/reduction; and (4) ozonolysis/reduction (Lligadas *et al*., 2013, Bockisch, *et al*., 2015, Lu *et al*., 2009). A successful chemically modification of plant oils to obtain polyols with considerable number of hydroxyl groups suitable for synthesis structural PUs must originally contain at least carbon-carbon double bonds, typically greater than 2.5 per triglyceride. Plant oil-based polyols are inexpensive, environment-friendly, available in large quantities, and renewable (Gogoi *et al*. 2014, Madbouly *et al*. 2013, Chowdhury *et al*. 2020, Zhang *et al*., 2015, Gaddam *et al*., 2018, Zafa *et al*., 2019). Castor oil was used previously to synthesis different polymers and polymer dispersions due to its hydroxyl group functionality. In addition, castor oil can be employed as an important chemical components in the synthesis of a bio-based nylon 11 (Winnacker *et al*. 2016).

Solventborne PU systems have been used widely in different applications, such as adhesive, coatings, paints, ink, etc. Large quantities of organic solvents normally evaporated to the atmosphere during the applications of these dispersions that normally cause air quality and environmental problems. Considerable efforts have been done by air quality regulators and Environmental Protection Agency to reduce the volatile organic compounds (VOCs) in the atmosphere and encourage industries to develop new environmentally friendly, bio-based products (Mishra *et al*., 2017, Mehravar, *et al*., 2019, Zhou *et al*., 2016, Song *et al*., 2017, Serkis *et al*. 2016). Aqueous polyurethane dispersions (PUDs) have been used in many industrial application as alternatives to their solvent-based due to the increasing pressure to limit detrimental environmental and health effects. In this case, no toxic VOCs used in the final products of PUDs but only water as a benign and environmentally friendly solvent.

The aqueous PUDs are the most rapidly developing branches of PU chemistry and driven by their versatility and environmental friendliness. The dispersions can be tailored to various industrial applications based on the method of preparation, nature of the polyols, diisocyanate, internal surfactant and ratio of hard to soft segments. For example, aqueous PUDs have been used as green coatings, adhesives, paint additives, pigment pasters, and others (Hakke *et al*., 2020, Akram *et al*., 2020, Xie *et al*., 2020). The early studies of Dieterich *et al*. on aqueous PUDs inspired much of the work of these dispersions (Dieterich *et al*., 1970, Dieterich, 1981). The nature of colloidal state, dispersion stability, particle-particle interaction, particle size and distribution are all important parameters and play very important roles on the performance of film formation.

Lignin is an abundant natural polymer found in all vascular plants between the cells and in the cell walls. Approximately 150 billion tons of lignin is produced by plants as the most abundantly natural polymer next to cellulose. Lignin is naturally hydrophobic with aromatic chemical structure composed of three different phenyl propane monomers (syringyl (S); guaiacyl (G); and p-hydroxyphenyl (H) subunits) (Zakzeski *et al*., 2010,). Lignin is biorenewable, environmentally friendly, low cost, $CO_2$ neutral, and antioxidant, stabilizer, and has antimicrobial properties compared to most petroleum-based materials (Dong *et al*., 2011). Regardless of the mentioned advantages industrial applications of lignin are limited due to its complex chemical structure

and its insolubility in common organic solvents (Sharma *et al*., 2020).

It also has been found that lignin could be surface modified and functionalized into new materials that can be employed in different applications (Liu *et al*., 2019, Wang *et al*., 2019, Zhang *et al*., 2018, Zhang *et al*., 2015, Li *et al*. 2017). For example, wide range of carbon-based materials were recently synthesized from different biomass including lignocellulosic hardwood, softwood, and agricultural waste (Yang *et al*., 2019). In addition, copolymers of lignin and poly(ε-caprolactone-*co*-lactide) have been successfully synthesized with different molecular weights and $T_{gs}$ with no organic solvent via ring-opening polymerization (Kai *et al*., 2017). Hierarchical porous with three-dimensional structure of lignin-based material was also created for applications of high-performance supercapacitor electrode. lignosulfonate (LS) is a water-soluble polyelectrolyte polymer (anionic) commonly obtained from the sulfite pulping of the brown or red liquor (Lebo *et al*., 2001). The LS can also be obtained with high yield from pulping liquid through ultrafiltration technique (Liu *et al*., 2020).

Thermoplastic and thermosetting shape-memory polymers and composites (SMPs) are widely used in manufacturing of medical devices, such as cardiac pacemakers, stents, surgical sutures, etc. (Lendlein *et al*., 2019, Bellin *et al*. 2006). The principle of shape-memory effect (SME) is based on the ability of material to temporarily stay in a certain deformed shape and then return to its permanent shape when exposed to external stimulus, such as heat, light, magnetic field (Jian *et al*., 2006, Lendlein *et al*. 2005, Santo *et al*. 2020). The thermal-induced SME is the most common one and can be obtained via direct heating (e.g. hot air, hot fluid, electric heater) or indirect heating (e.g. exposure to light, exothermic reaction, or an alternating magnetic field) (Madbouly *et al*. 2012, Kratz *et al*. 2011, Madbouly *et al*., 2009). For biomedical applications, the SMPs will be fixed in their compressed temporary shape after that they will be implanted and then they will be recovered to their original shape inside the body. Biodegradability of SMPs is an additional desire function for certain applications allowing completely biodegradation of the materials in the boy without a need for a second surgery for device explantation. Programming of SMPs is a process based on combination of a suitable polymer morphology/architecture with a thermomechanical procedure. The permanent shape of the SMPs is defined by physical or chemical cross-links and prevent polymers to flow at high temperatures. The temporary shape can be fixed by the solidification of switching domains either by vitrification or crystallization or by a low $T_g$. The SMPs can be recovered to their original permanent shapes by heating the deformed samples under zero force. The temperature must be exceeded the switching temperature $T_{sw}$ associated with the thermal transition $T_{trans}$ of the switching soft domains. In general, the SME can be summarized based on the following steps: (i) using conventional processing techniques, such as extrusion and/or injection molding to create the permanent shape of the SMP (ii) Increase the temperature of the SMP to $T_{high} > T_{trans}$ and deform it to $e_m$; (iii) cool the sample down to $T_{low} < T_{trans}$ while keeping the stress $s_m$ obtained at $e_m$ constant. After removing the external stress, the temporary shape of the SMP can be obtained. The permeant original shape cab be recovered by heating the sample to $T_{high}$.

The chemical structure of LS has several hydroxyl groups suitable for polyurethane synthesis through reaction with diisocyanate. Therefore, the goal of this current manuscript is to synthesis a new castor oil-based PUDs with different concentrations of LS that will be chemically copolymerized with diisocyanate similar to the reaction of castor oil polyols. It is expected that LS can significantly improve the thermomechanical properties, shape-memory effect, biocompatibility, and the ability of the cast film to form three-dimensional porous structure with supper critical carbon dioxide. This current study is a continuation to our previous series of study and contribution of aqueous bio-based polyurethane dispersions and nanocomposites (Zhang *et al*., 2017, Madbouly *et al*., 2009, Madbouly *et al*., 2006).

## Experimental section

### Materials

The castor oil, sodium LS, DMPA, dibutyltin dilaurate (DBTDL), and isophorone diisocyanate (IPDI) were obtained from Aldrich Chemical Co. (Milwaukee, WI). The methyl ethyl ketone (MEK) and triethylamine (TEA) were purchased

from Fisher Scientific Company (Fair Lawn, NJ). The materials used as received without additional analysis or treatment.

### Synthesis of castor oil-based PU−LS aqueous dispersions

The castor oil, IPDI, DMPA, and one drop of DBTDL as a catalyst were mixed at 78 °C for 1 h in a three-necked flask reactor. Different weights of LS were added to the mixture to prepare 1, 3, 5, and 7 wt.% LS. While the total concentration of the polymer solid in liquid water was kept at 15 wt.%, the molar ratio between NCO in IPDI, the OH in castor oil and LS, and the OH in DMPA was kept at 2.0:1.0:0.99. After 2 h reaction time, the TEA (3 equiv. per DMPA) was added to neutralize the free carboxylic acid groups. The water was added over 30 min (dropwise) under 600 rpm agitation speed. The MEK was then removed and PUDs with no organic solvent obtained. All the dispersions were prepared with a solid content of ≈15 wt.%, as mentioned above. Figure 1 shows the elementary steps for the synthesis of castor oil-based PU−LS dispersion.

### Rheological measurements and transmission electron microscopy

The dynamic viscosity of PUDs as a function of LS content at 20 °C was measured using an AR2000ex rheometer (TA Instruments) with 25 mm diameter parallel plates. The measurments were carried out at 1% strain in the linear viscoelastic regime, and 0.1 to 100 rad/s angular frequency. A thin layer of low-viscosity silicone oil was applied to the air/sample interface to eliminate any evaporation of the liquid water during the measurements.

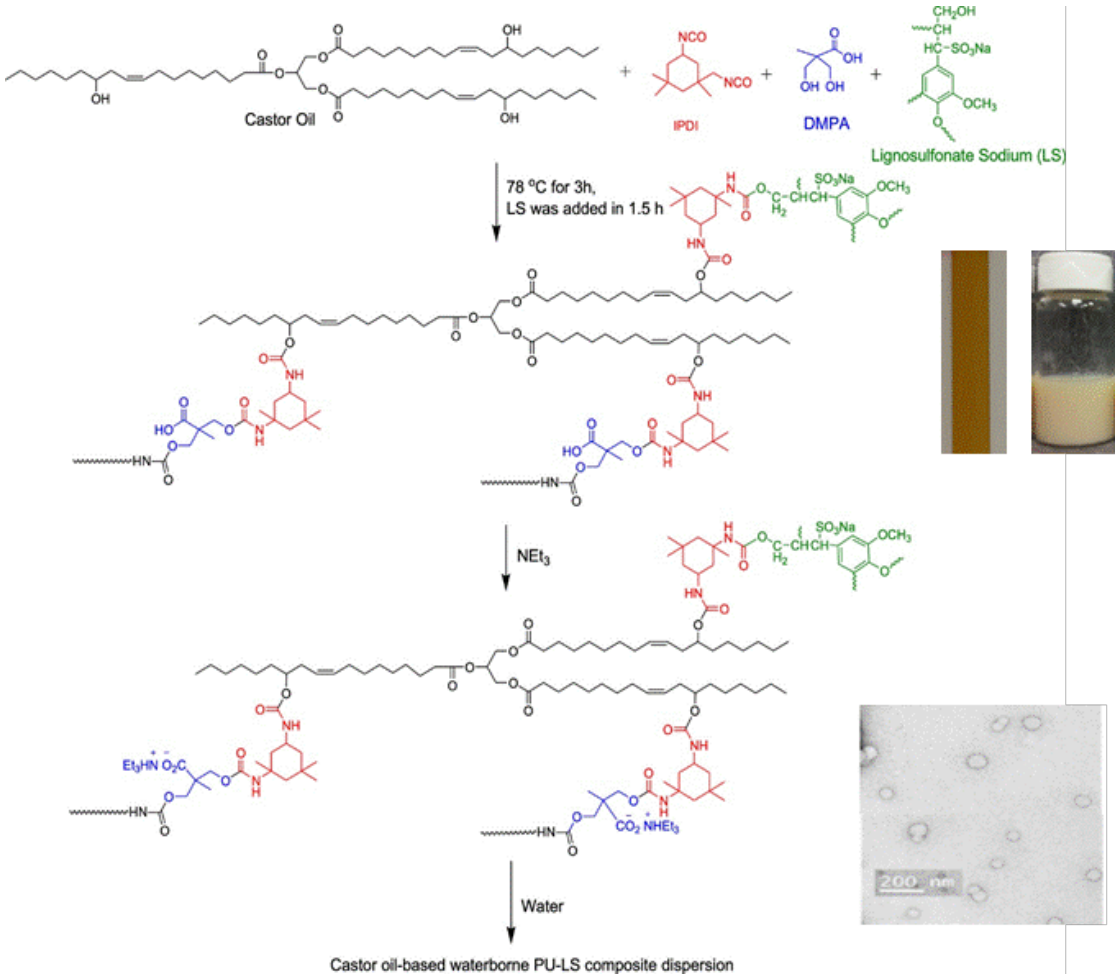


**Figure 1.** Elementary steps for the synthesis of castor oil-based PU-LS dispersion. The TEM picture is for 5 wt.% LS dispersion and the glass jar shows a picture of the aqueous dispersion.

The morphology of the dispersions or particle size analysis was investigated using Transmission Electron Microscopy, TEM (1200EX by JEOL, Ltd.) the dispersion must be diluted to 0.5 solid wt.% using DI water to obtain successful particle size analysis. After that , a 3 ml small drop of the diluted dispersion was deposited onto a TEM carbon film grid. Excess deposited dispersion can be removed from the TEM grid using a filter paper. Approximately 2 wt.% aqueous uranium acetate solution was used as a negative stain agent for better contrast.

### Cast-film preparation, DSC, and DMA measurements

The PU-LS films of different LS contents were obtained via dispersion casting process. The dispersions casted onto a polypropylene plate at room temperature. The films were obtained after drying at room temperature for 2 days and under vacuum at 60 °C for another 2 days. About 0.77 mm thick samples for all dispersions were obtained.

The DSC measurements were investigated using a TA Instruments Q2000. The $T_{gs}$ of the casted PU-LS films were determined at 10 °C/min heating rate under dry nitrogen atmosphere. The $T_{gs}$ were evaluated accurately from the temperature at the half of the step height in a specific heat curve.
The TA Q800 dynamic mechanical analyzer, was employed for the DMA measurements for all PU-LS films. The measurments were carried out for rectangular-shaped samples of 0.77 mm thickness and 8 mm width from − 90 °C to 100 °C at 2 °C/min heating rate and 1 Hz frequency under a nitrogen atmosphere. The DMA measurements are used to evaluate the effect of LS on the glass-relaxation process of castor oil-based PU−LS samples. The $T_{gs}$ of the films were obtained from the temperature at the peak maximum of the tan δ curves.

### Foam process and SEM morphology

The samples of different LS contents were saturated with supercritical carbon dioxide ($scCO_2$) at 25 °C and 100 bar for 20 min in a pressure vessel. The foam structure was created as a result of nucleation and expansion of dissolved $CO_2$ during the high depressurization rate. The obtained foam was stabilized at low temperature (10 °C) for 12 hours. The morphology of the PU-LS foams was investigated using scanning electron microscopy (SEM). Surface fractured of the foams were carried out in liquid nitrogen, then the samples were fixed on special SEM holders, and sputtered with gold. The morphology of the foams were investigated using a field emission scanning electron microscope (FE-SEM, FEI Quanta 250) at 10 kV in a high vacuum chamber.

### Thermomechanical shape-memory cycles:

The shape memory properties were investigated using the TA Instruments Q800 dynamic mechanical analyzer. Thermomechanical cycle was employed to investigate the shape memory effect (SME) of PU-LS of different concentrations. The samples were heated up to the programming temperature, $T_{prog}$ =37 °C and held at this temperature for 2 min equilibrium time. The samples were stretched to 100% maximum strain ($\varepsilon_m$) at a rate of 10%/min. The samples were then cooled down to $T_{low}$ = -20 °C at 10 °C/min cooling rate under the applied stress and holding for 10 min. Finally, the temperature was increased to $T_{high}$ at a rate of 3 °C/min and held at this temperature for 30 min to recover a fixed strain ($\varepsilon_p$).recovery time. The values of $T_{prog}$, $T_{low}$, $T_{high}$ based on the different $T_g$ values of the samples will be discussed later.

### Results and discussion

The rheological behavior of PU-LS dispersion was found to be strongly influenced by the LS content. Figure 2 depicts the composition dependence of PU-LS dispersion of dynamic shear moduli, *G'* and *G''* as well as complex viscosity, $\eta^*$ at 20 °C. Clearly both *G', G'',* and $\eta^*$ are strongly increased with increasing the LS content as clearly seen in Figure 2. The significant increase in the rheological properties (*G', G'',* and $\eta^*$) of PU−LS dispersions with increasing content of LS can be attributed to several reasons. The first one is the particle size of PU-LS in the aqueous dispersion. The TEM investigation revealed that all the PU-LS dispersions with different LS contents have almost the same particle size (35 nm) as clearly seen in figure 2. Therefore, the particle size plays no role in the increase of the *G', G'',* and $\eta^*$. It must be mentioned here that the concentration of DMPA (internal surfactant) and the neutralizing agent (TEA) are exactly the same

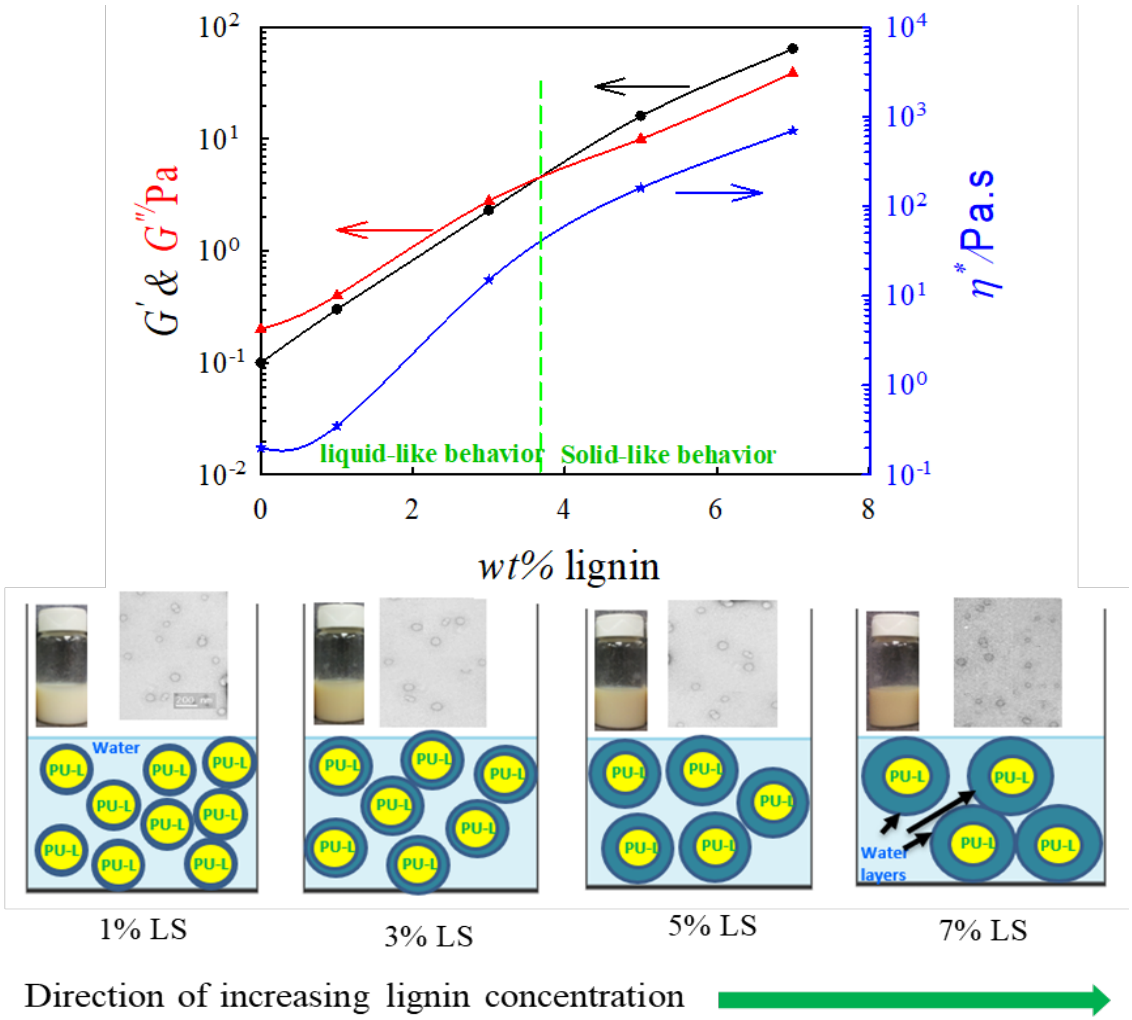


**Figure 2.** Lignin composition (LS) dependence of shear moduli, *G'* and *G''* and complex viscosity, η* at 20 °C. Waterborne PU–LS dispersions and their TEM photographs for different LS concentrations. Schematic diagram for PU-LS dispersion with different contents of LS. The thickness of the water layer on the surface of PU-LS nanoparticles increases with increasing concentration of LS, as clearly described by the arrow.

for all PU-LS dispersions. Therefore, all particles should have similar ionic charges regardless of the different concentration of LS. In addition, the TEM photographs were taken after dilution of the dispersions with DI water to 0.5 wt.%, as mentioned in the Experimental Section. A small drop of approximately 3 µL was then taken from the diluted dispersion and deposited onto the TEM grid to form a thin layer. A filter paper was used to remove the water excess from the TEM grid. Therefore, the TEM technique cannot provide any information about the thickness of the water layer surrounding the PU−LS nanoparticles. Based on the above discussion, it appears that the main reason for the increase in *G'*, *G''*, and η* with increasing lignin content is the chemical structure and water affinity of LS. As shown in Figure 1, the LS is soluble in water due to its salt-like chemical structure with hydrophilic and hydrophobic functional groups. The LS can react with the IPDI via the hydroxyl groups in the LS and become a part of the PU backbone that will be dispersed in water.

The PU-LS can form stable dispersions only when the PU-LS nanoparticles are uniformly dispersed in the continuous water phase. However, on the other hand unstable PU-LS dispersion can be obtained in the case that the PU-LS particles coalesce and form larger droplets with a considerable decrease in the surface area. Flocculation is another form of unstable dispersion commonly occurs in dispersions

when the particles aggregate without making a new particle. No sign of dispersion instability or particle aggregation or flocculation has been observed in the PU-LS aqueous dispersions as seen in the TEM photographs of PU-LS dispersions of different LS contents as already mentioned above. The hydrophobic nature of the LS leads to the fact that the PU-LS nanoparticle adsorbs more water molecules onto the surface than that of the castor oil-based PU dispersion with no lignin. With increasing the lignin content, the thickness of the water layer absorbed on the PU-LS nanoparticles increases. Therefore, with keeping the numbers of the PU-LS nanoparticles constant, the water thick layer leads to a significant decrease in the continuous water phase with increasing the lignin content, and consequently a dramatic increase in the *G', G",* and $\eta^*$ was observed as clearly seen in Figure 2.

The LS was found to have a considerable influence on the glass transition temperature of the cast PU-LS film as illustrated in the thermograms in Figure 3a. The $T_g$ was determined from the temperature of half of the step height in specific heat curves (see the arrows in Figure 3a). The $T_g$ of pure castor oil-based PU with no lignin is about 9.7 °C. The $T_g$ increases by almost double ($T_g$ = 18.6 °C) with 3 wt.% LS due to the highly aromatic rigid structure of LS. For higher LS contents (higher than 3 wt.%), the $T_g$ of the PU-LS was almost constant regardless the increase in the LS content. Figure 3b shows the temperature dependence of tan $\delta$ for PU-LS films obtained from the solvent cast of the dispersions. The inset plot of Figure 3b shows the temperature dependence of the storage modulus ($E'$).

The peak maximum of tan $\delta$ is related to Micro-Brownian cooperative relaxation process of the main polymer chain (α–relaxation) process and related to the $T_g$ of the PU-LS films. For PU-LS films with LS ≤ 3 wt. %, the $T_g$ obtained from the tanδ peak maximum increases with increasing concentration of LS. Both tan $\delta$ and $E'$ reached constant values regardless of the content of LS for higher LS concentrations. The plateau of $E'$ at $T \geq 90$ °C (i.e., $E'$ is temperature-independent) is related to the cross-link dentistry of the PU-LS films. In principle the cross-link density can be evaluated from the plateaus or the rubbery moduli at 40 °C above the $T_g$ of each composition based on the rubber elasticity theory using the following equation (ward *et al*. 1971):

$$E' = 3\upsilon_e RT \quad (1)$$

Where $E'$ is the storage modulus at 40 °C above $T_g$, $\upsilon_e$ is the cross-link density, $T$ is the absolute temperature, and $R$ is the universal gas constant. The cross-link densities of PU-LS films increase from 123.7 mol/m$^{-3}$ for castor oil-based PU with no LS to 208.7 mol/m$^{-3}$ for PU-LS with LS content from 0 to 7 wt.%. This experimental fact is attributed to the rigid structure of LS, which provides more stability to the cross-linked films and consequently, the cross-link density increases.

Porous structure or scaffold can be fabricated with many techniques including solvent cast/salt leaching (Mikos *et al*., 1994) phase separation, (Lo *et al*., 1995) fabric foaming processing (Freed *et al*., 1994) fiber extrusion and gas foaming (Singh *et al*., 2004) as well as $scCO_2$ method (Tai *et al*., 2007). The $scCO_2$ has a great advantage compared to the other techniques due to its high efficiency for creating highly interconnected porous structure in relatively short saturation times. Normally the polymer will be saturated with

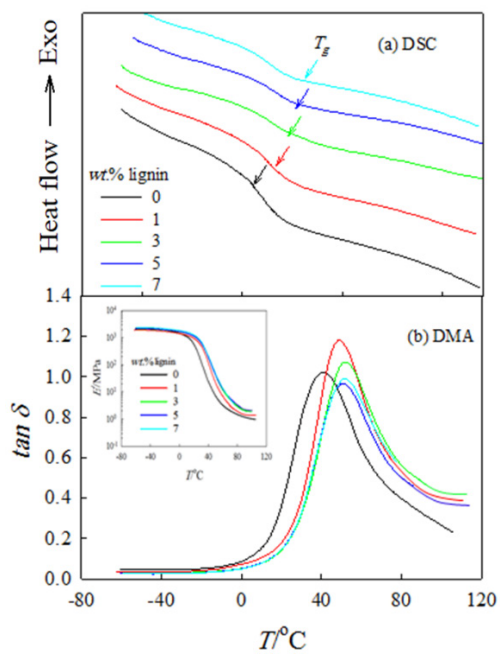


**Figure 3. (a)** DSC thermograms for PU-LS films of different lignin (LS) contents, the arrows show the $T_{gs}$ of the films. **(b)** Temperature dependence of tan $\delta$ for PU–LS with different LS contents. The inset plot of Figure 3 (b) shows the temperature dependence of storage modulus, $E'$ for different LS contents.

$scCO_2$ at pressure and elevated temperature for certain saturation time, then the porous structure will be generated when the high pressure will be depressurized at high rate, where the nucleation and expansion of dissolved $CO_2$ making the foam. The foaming temperature, saturation time and depressurization rate are the most important factors commonly used to control porosity, pore size, distribution of pores, and density. The $scCO_2$ foaming technique is environmentally friendly, where no usage of volatile organic compounds in the foaming process. The PU-LS films with different LS contents obtained from dispersions cast can be used to fabricate porous structure via $scCO_2$ foaming technique. The SEM photographs of PU-LS foams of different LS contents are shown in Figure 4. Clearly the average pore size was found to be LS content dependent. The higher the concentration of LS the lower the pore size. The average pore size of castor oil-based PU (no LS) foam was decreased from about 70 µm to approximately 30 µm for PU-LS with 7 wt.% LS. The degree of porosity of all samples was about 85% based on the pycnometry measurements, 10% of the pores were accessible by nitrogen. The lower size of the pores with increasing the LS contents might be attributed to the rigid structure and the high $T_g$ and viscosity of the films with high contents of LS. This porous structure could be suitable for biomedical applications if the PU-LS is biocompatible. The cytotoxicity tests of PU-LS sample with comparison with other PCL-based polymers will be studied in another manuscript.

## Shape memory effect

Active movement with respect to changing temperatures (i.e., thermally induced-SME) is an important characteristic parameter for creating smart PU-LS multifunctional films. The SME of PU-LS films obtained from the dispersion cast method were carried out using cyclic thermomechanical tensile tests. The tests were performed by stretching the samples to 100% $\varepsilon_m$ at $T_{prog}$ of 37 °C and rapidly cooled down to $T_{low}$ = –20 °C. Cooling the SMP samples to $T_{low}$ = –20 °C must be occurred under the applied stress to efficiently fix the temporary shape. The temporary shape will be fixed by the $T_g$ of the PU-LS sample. The crosslink nature of all PU-LS films act as permanent net points determining the permanent shape. The recovery of all samples to its original permanent shapes was recorded by heating the sample at 2 °C/min heating rate up to 70 °C. The recovery module was applied under stress-controlled condition in this manuscript. A typical cyclic thermomechanical measurement for castor oil-based PU film with no LS under stress-controlled condition is shown in Figure 5 shows.

The cyclic thermomechanical tensile tests for PU-LS films of different LS contents under

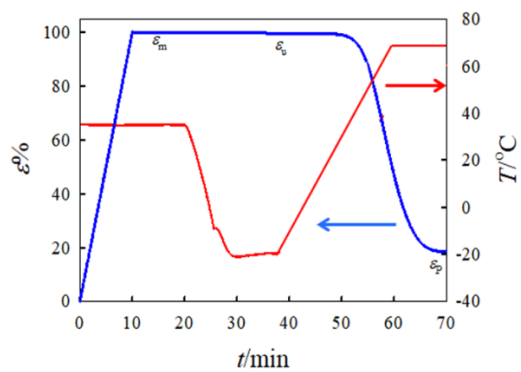


**Figure 5.** DMA thermomechanical cycle (stress control) as time dependence of ε% and temperature for the castor oil-based PU film. The measurement was carried out at $T_{prog}$ = 37 °C, $\varepsilon_m$ = 100%, $T_{low}$ = –20 °C, and $T_{high}$ = 70 °C

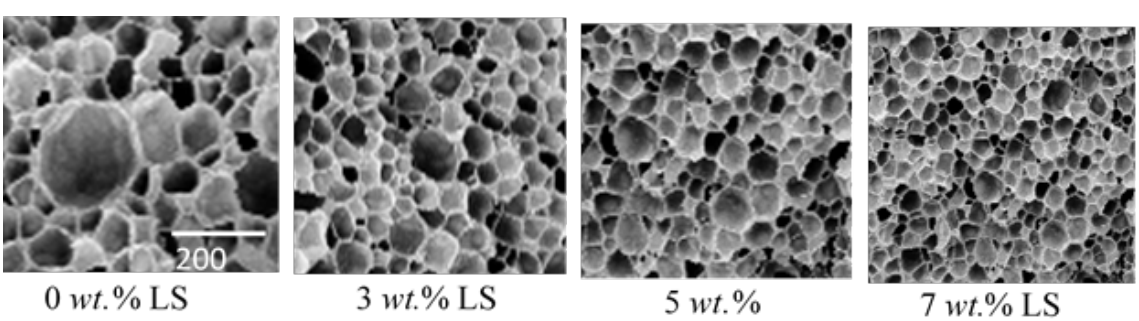


**Figure 4.** SEM morphologies for PU-LS films of different LS contents. The porous structure was created using scCO2 technique at 25 °C and 100 bar for 20 min.

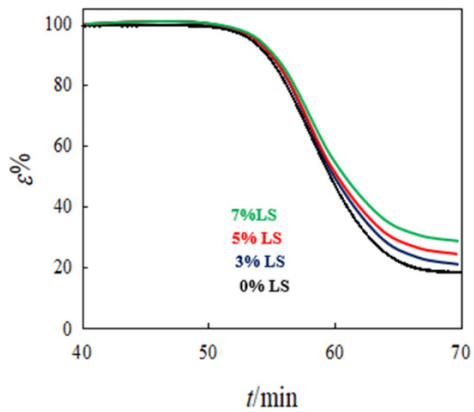


**Figure 6.** The ε% for PU-LS films of different LS contents as a function of recovery time. The thermo-mechanical cyclic tests were investigated at $T_{prog}$ = 37 °C, $\varepsilon_m$ = 100%, $T_{low}$ = -20 °C, and $T_{high}$ = 70 °C.

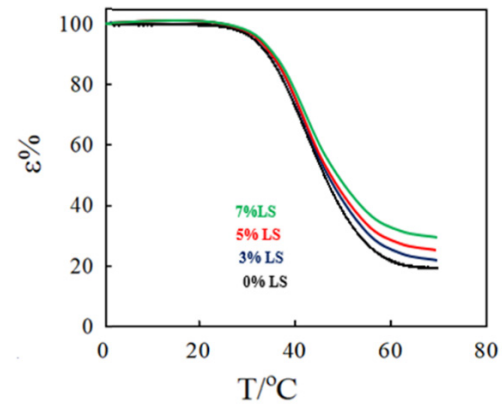


**Figure 7.** Temperature dependence of ε% for PU-LS films of different LS contents. The thermo-mechanical cyclic tests were investigated at $T_{prog}$ = 37 °C, $\varepsilon_m$ = 100%, $T_{low}$ = -20 °C, and $T_{high}$ = 70 °C.

stress-controlled condition is shown in Figure 6. Clearly the LS has a significant impact on the shape fixity rate, $R_f$, shape recovery rate, $R_r$, and $T_{sw}$. The value of $R_r$ can be calculated from the deformation in the temporary shape $e_u$ and the extension at the stress-free state after recovery $e_p$ (N) from two subsequent cycles (N-1) and $N$ according to the following equation (Madbouly *et al*. 2012, Kratz *et al*. 2011, Madbouly *et al*., 2009):

$$R_r(N) = \frac{\varepsilon_u(N)-\varepsilon_p(N)}{\varepsilon_u(N)-\varepsilon_p(N-1)} \quad (2)$$

The value of $R_f$ can be calculated for cycle $N$ according to the Equation (3):

$$\varepsilon_f(N) = \frac{\varepsilon_u(N)}{\varepsilon_m} \quad (3)$$

For all PU-LS with different LS contents, the value of $R_f$ was found to be approximately 99%.

The temperature dependence of ε% for PU-LS of different LS contents is shown in Figure 7. Clearly $R_r$ decreases systematically from 80% for castor oil-based PU film with no LS to 70% for PU-LS with 7 wt.% LS. The decrease in $R_r$ with increasing LS content is mainly attributed to the high stiffness of LS compared to the pure castor oil-based PU film.

To demonstrate the SME for the PU-LS solid film obtained from their aqueous dispersion with 5 wt.% LS, a plane stripe sample was folded at a program temperature of 37 °C and the temporary shape was fixed by cooling the sample in an ice

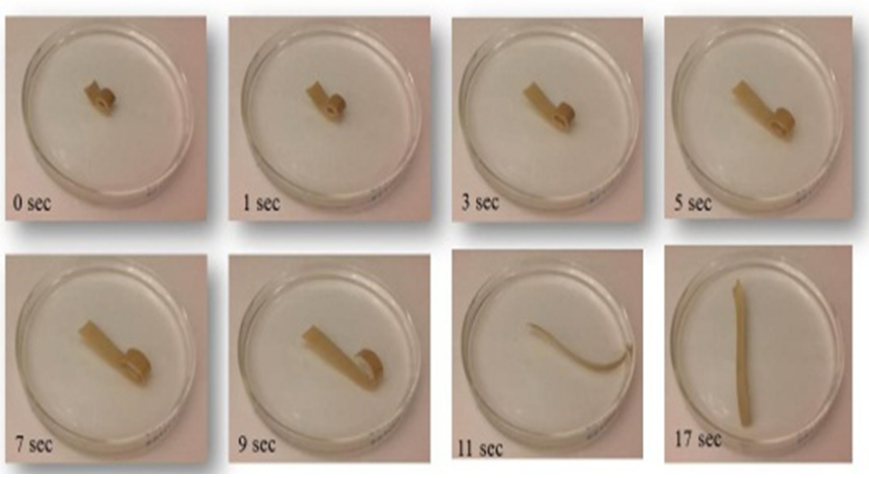


**Figure 8.** Thermal-induced SME of PU-LS with 5 wt.% LS. The folded temporary shape changes quickly (17 sec) to its plane stripe permanent shape (100% recovery) once the sample immersed in a petri-dish with hot water at 37 °C.

water bath. The temporary folded shape changed to its permanent shape (plane stripe) within just 17 s once the sample was immersed in a water bath at 37 $^{o}$ C as clearly shown in Fig. 8.

## Conclusion

Aqueous bio-based dispersions based on castor oil and LS were successfully synthesized with nanoscale dispersions as small as 35 nm with excellent dispersion stability of different LS contents. Incorporation of small concentration of LS was found to have strong positive impact of both dispersion behavior and solid films. Transparent thin films of PU-LS with different concentrations of LS were obtained via solution (dispersion) cast technique. The dynamic viscosity of the PU-LS was increased dramatically with increasing the concentration of LS with keeping the solid content constant at 15 wt.% for all dispersions. This experimental fact was attributed to the nature of the chemical structure of LS. The LS is a water-soluble material and reacted with diisocyanate similar to the polyols. Therefore, lignin is a part of the dispersion particle (i.e., the nanoparticles is in fact a mixture (copolymer) of polyurethane and lignin dispersed in water). Therefore, the PU-LS nanoparticle can adsorb thick water layer with increasing the LS content. Therefore, the free water in the dispersion would significantly decrease and consequently the dispersion viscosity increases. The $T_{gs}$ of the PU-LS films were measured from the temperature of the tan δ peak maximum. The $T_g$ was found to be increased with increasing the LS content up to 3 wt.% LS. For high LS content, no additional increase in $T_g$ was observed. The cross-link density was evaluated from the storage modulus plateau at 40 $^{o}$C above the $T_g$ using DMA measurments based on the theory of rubber elasticity. The PU-LS films were used to fabricate porous structure using $scCO_2$. The average pore size was found to be LS content dependent. The higher the concentration of LS the lower the pore size. The average pre size of castor oil-based PU (no LS) foam was decreased from about 70 µm to approximately 30 µm for PU-LS with 7 wt.% LS. The PU-LS films were found to have excellent thermally induced shape-memory effect. The rate of shape recovery decreases systematically from 80% for pure castor oil-based PU film with no LS to 70% for PU-LS with 7 wt.% LS. The decrease in the shape recovery with increasing LS content is mainly attributed to the high stiffness of LS compared to the pure castor oil-based PU film.

## Data statement

All the data reported in this manuscript will be made availale via Cranfield open repository.

## Conflict of interest

The authors declare to have no conflict of interest.

## References

Akram, N., Zia, K.M., Saeed, M., Khosa, M.K., Khan, W.G. and Arain, M.A. (2020). Compositional effect on the deformation behavior of polyurethane pressure-sensitive adhesive thin films. *Journal of Applied Polymer Science*, *137*(8), p.48395.

Andjelkovic, D. D.; Larock, R. C. (2006). Novel Rubbers from cationic copolymerization of soybean oils and dicyclopentadiene. 1. Synthesis and characterization. *Biomacromolecules 7*, 927–936,

Araby, S., Philips, B., Meng, Q., Ma, J., Laoui, T. and Wang, C.H. (2021). Recent advances in carbon-based nanomaterials for flame retardant polymers and composites. *Composites Part B: Engineering*, p.108675

Bellin, I., Kelch, S., Langer, R. and Lendlein, A. (2006) Polymeric triple-shape materials. *Proceedings of the National Academy of Sciences*, *103*(48), pp.18043-18047.

Bockisch, M. (2015). *Fats and oils handbook (Nahrungsfette und Öle)*. Elsevier.

Chowdhury, R. A.; Clarkson, C. M.; Shrestha, S.; El Awad Azrak, S. M.; Mavlan, M.; Youngblood, J. P. (2020) High-Performance Waterborne Polyurethane Coating Based on a Blocked Isocyanate with Cellulose Nanocrystals (CNC) as the Polyol. *ACS Appl. Polym. Mater. 2*, 385–393.

Dahy, H. (2017). Biocomposite materials based on annual natural fibres and biopolymers–Design, fabrication and customized applications in architecture. *Construction and Building Materials*, *147*, pp.212-220.

Dieterich, D., Keberle, W. and Wuest, R. (1970). Aqueous dispersions of polyurethane ionomers. *Journal Of The Oil & Colour Chemists Association*, *53*(5), pp.363-379.

Dieterich, D. (1981). Aqueous emulsions, dispersions and solutions of polyurethanes; synthesis and properties. *Progress in Organic Coatings*, *9*(3), pp.281-340.

Dong, X., Dong, M., Lu, Y., Turley, A., Jin, T. and Wu, C. (2011). Antimicrobial and antioxidant activities of lignin from residue of corn stover to ethanol production. *Industrial Crops and Products*, *34*(3), pp.1629-1634.

El-Sherbiny, I.M. and Ali, I.H. (2017). Biopolymer-Based Nanocomposites for Environmental Applications. *Handbook of Composites from Renewable Materials, Nanocomposites: Advanced Applications*, *8*, p.389.

Freed, L.E., Vunjak-Novakovic, G., Biron, R.J., Eagles, D.B., Lesnoy, D.C., Barlow, S.K. and Langer, R. (1994). Biodegradable polymer scaffolds for tissue engineering. *Bio/technology*, *12*(7), pp.689-693.

Gaddam, S. K.; Palanisamy, A. (2018). Effect of counterion on the properties of anionic waterborne polyurethane dispersions developed from cottonseed oil-based polyol. *J. Polym. Res. 25*, 1–86.

Gandini, A.; Lacerda, T. M.; Carvalho, A. J. F.; Trovatti, E. (2016). Progress of polymers from renewable resources: furans, vegetable oils, and polysaccharides. *Chem. Rev. 116*, 1637–1669,

Gogoi, S.; Karak, N. (2014). Bio-based biodegradable waterborne hyperbranched polyurethane as an ecofriendly sustainable material. *ACS Sustain. Chem. Eng.*, *2*, 2730–2738.

Gutiérrez, T.J. and Alvarez, V.A. (2017). Cellulosic materials as natural fillers in starch-containing matrix-based films: a review. *Polymer Bulletin*, *74*(6), pp.2401-2430.

Hakke, V.S., Bagale, U.D., Boufi, S., Babu, G.U.B. and Sonawane, S.H. (2020). Ultrasound Assisted Synthesis of Starch Nanocrystals and It's Applications with Polyurethane for Packaging Film. *Journal of Renewable Materials*, *8*(3), p.239.

Hussain, N., Bilal, M. and Iqbal, H.M. (2022). Carbon-based nanomaterials with multipurpose attributes for water treatment: Greening the 21st-century nanostructure materials deployment. *Biomaterials and Polymers Horizon*, *1*(1), pp.48-58.

Ionescu, E., Bernard, S., Lucas, R., Kroll, P., Ushakov, S., Navrotsky, A. and Riedel, R. (2021). Polymer-derived ultra-high temperature ceramics (UHTCs) and related materials. *Ceramics, Glass and Glass-Ceramics*, pp.281-323.

Jamróz, E., Kulawik, P. and Kopel, P. The effect of nanofillers on the functional properties of biopolymer-based films: A review. *Polymers*, *11*(4), p.675, 2019. https://www.mdpi.com/2073-4360/11/4/675

Jiang, H.Y., Kelch, S. and Lendlein, A. (2006). Polymers move in response to light. *Advanced Materials*, *18*(11), pp.1471-1475.

Jiménez, A.M., Espinach, F.X., Delgado-Aguilar, M., Reixach, R., Quintana, G., Fullana-i-Palmer, P. and Mutjé, P. (2016). Starch-based biopolymer reinforced with high yield fibers from sugarcane bagasse as a technical and environmentally friendly alternative to high density polyethylene. *BioResources*, *11*(4), pp.9856-9868.

Kai, D.; Zhang, K.; Jiang, L.; Wong, H. Z.; Li, Z.; Zhang, Z.; Loh, X. J. (2017) Sustainable and antioxidant lignin–polyester copolymers and nanofibers for potential healthcare applications. *ACS Sustainable Chem. Eng. 5*, 6016–6025.

Kratz, K., Madbouly, S.A., Wagermaier, W. and Lendlein, A. (2011) Temperature-memory polymer networks with crystallizable controlling units. *Advanced Materials*, *23*(35), pp.4058-4062.

Kumar, A., Sood, A. and Han, S.S. (2022). Potential of magnetic nano cellulose in biomedical applications: Recent Advances. *Biomaterials and Polymers Horizon*, *1*(1), pp.1-16.

Kundu, P. P.; Larock, R. C. Novel conjugated linseed oil-styrene-divinylbenzene copolymers prepared by thermal polymerization. 1. (2005). Effect of monomer concentration on the structure and properties. *Biomacromolecules 6*, 797–806,

Lligadas, G., Ronda, J.C., Galia, M. and Cadiz, V., 2013. (2013) Renewable polymeric materials from vegetable oils: a perspective. *Materials today*, *16*(9), pp.337-343.

Lebo, S. E., Jr.; Gargulak, J. D.; McNally, T. J. (2001). Lignin″. *Kirk-Othmer Encyclopedia of Chemical Technology*.

Lendlein, A. and Gould, O.E.(2019). Reprogrammable recovery and actuation behaviour of shape-memory polymers. *Nature Reviews Materials*, *4*(2), pp.116-133.

Lendlein, A., Jiang, H., Jünger, O. and Langer, R. (2005). Light-induced shape-memory polymers. *Nature*, *434*(7035), pp.879-882.

Liu, F.; Zhang, Z.; Wang, Z.; Dai, X.; Chen, M.; Zhang, J. (2020). Novel lignosulfonate/N, N-dimethylacrylamide/γ-methacryloxypropyl trimethoxy silane graft copolymer as a filtration reducer for water-based drilling fluids. *J. Appl. Polym. Sci. 137*, 48274.

Li, H.; Sun, J.-T.; Wang, C.; Liu, S.; Yuan, D.; Zhou, X.; Tan, J.; Stubbs, L.; He, C. (2017). High modulus, strength, and toughness polyurethane elastomer based on unmodified lignin. *ACS Sustainable Chem. Eng. 5*, 7942–7949.

Liu, W.; Fang, C.; Wang, S.; Huang, J.; Qiu, X. (2019). High- Performance Lignin-Containing Polyurethane Elastomers with Dynamic Covalent Polymer Networks. *Macromolecules 52*, 6474–6484.

Lo, H., Ponticiello, M.S. and Leong, K.W. (1995). Fabrication of controlled release biodegradable foams by phase separation. *Tissue engineering*, *1*(1), pp.15-28.

Lu, Y. and Larock, R.C. (2009). Novel polymeric materials from vegetable oils and vinyl monomers: preparation, properties, and applications. *ChemSusChem: Chemistry & Sustainability Energy & Materials*, *2*(2), pp.136-147.

Madbouly, S.A. and Lendlein, A.(2012). Degradable polyurethane/soy protein shape-memory polymer blends prepared via environmentally-friendly aqueous dispersions. *Macromolecular materials and engineering*, *297*(12), pp.1213-1224.

Madbouly, S.A. and Lendlein, A. (2009). Shape-memory polymer composites. In *Shape-Memory Polymers* (pp. 41-95). Springer, Berlin, Heidelberg.

Madbouly, S. A.; Otaigbe, J. U. (2009). Recent advances in synthesis, characterization and rheological properties of polyurethanes and POSS/polyurethane nanocomposites dispersions and films. *Prog. Polym. Sci. 34*, 1283–1332.

Madbouly, S. A.; Otaigbe, J. U. (2006). Kinetic analysis of fractal gel formation in waterborne polyurethane dispersions undergoing high deformation flows. *Macromolecules 39*, 4144–4151.

Madbouly, S. A.; Xia, Y.; Kessler, M. R. (2013). Rheological Behavior of Environmentally friendly castor oil-based waterborne polyurethane dispersions. *Macromolecules 46*, 4606–4616.

Mehravar, S., Ballard, N., Tomovska, R. and Asua, J.M. (2019). Polyurethane/Acrylic Hybrid Waterborne Dispersions: Synthesis, Properties and Applications. *Industrial & Engineering Chemistry Research*, *58*(46), pp.20902-20922.

Mikos, A.G., Thorsen, A.J., Czerwonka, L.A., Bao, Y., Langer, R., Winslow, D.N. and Vacanti, J.P. (1994). Preparation and characterization of poly (L-lactic acid) foams. *Polymer*, *35*(5), pp.1068-1077.

Mittal, D., Kumar, A., Balasubramaniam, B., Thakur, R., Siwal, S.S., Saini, R.V., Gupta, R.K. and Saini, A.K., (2022). Synthesis of Biogenic silver nanoparticles using plant growth-promoting bacteria: Potential use as biocontrol agent against phytopathogens. *Biomaterials and Polymers Horizon*, *1*(1), pp.1-10.

Mishra, V., Desai, J. and Patel, K.I. (2017). High-performance waterborne UV-curable polyurethane dispersion based on thiol–acrylate/thiol–epoxy hybrid networks. *Journal of Coatings Technology and Research*, *14*(5), pp.1069-1081.

Mishra, R.K., Goel, S. and Nezhad, H.Y. (2022). Computational prediction of electrical and thermal properties of graphene and BaTiO3 reinforced epoxy nanocomposites. *Biomaterials and polymers horizon*, *1*(1), pp.1-14.

Mowafi, S., El-Sayed, H. and Abou Taleb, M. (2018). Utilization of proteinic biopolymers: Current status and future prospects. *Journal of Textiles, Coloration and Polymer Science*, *15*(1), pp.15-31.

Santo, L., Quadrini, F., Bellisario, D. and Iorio, L. (2020). Applications of Shape-Memory Polymers, and Their Blends and Composites. *Shape Memory Polymers, Blends and Composites* (pp. 311-329). Springer, Singapore.

Sharma, S., Sharma, A., Mulla, S.I., Pant, D., Sharma, T. and Kumar, A.(2020). Lignin as Potent Industrial Biopolymer: An Introduction. In *Lignin* (pp. 1-15). Springer, Cham.

Serkis, M., Špírková, M., Hodan, J. and Kredatusová, J. (2016). Nanocomposites made from thermoplastic waterborne polyurethane and colloidal silica. The influence of nanosilica type and amount on the functional properties. *Progress in Organic Coatings*, *101*, pp.342-349.

Shi, S.C. and Lu, F.I. (2016). Biopolymer green lubricant for sustainable manufacturing. *Materials*, *9*(5), p.338.

Singh, L., Kumar, V. and Ratner, B.D. (2004). Generation of porous microcellular 85/15 poly (DL-lactide-co-glycolide) foams for biomedical applications. *Biomaterials*, *25*(13), pp.2611-2617.

Song, S.C., Kim, S.J., Park, K.K., Oh, J.G., Bae, S.G., Noh, G.H. and Lee, W.K. (2017). Synthesis and properties of waterborne UV-curable polyurethane acrylates using functional isocyanate. *Molecular Crystals and Liquid Crystals*, *659*(1), pp.40-45.

Tai, H., Mather, M.L., Howard, D., Wang, W., White, L.J., Crowe, J.A., Morgan, S.P., Chandra, A., Williams, D.J., Howdle, S.M. and Shakesheff, K.M. (2007). Control of pore size and structure of tissue engineering scaffolds produced by supercritical fluid processing. *Eur Cell Mater*, *14*, pp.64-77.

Visakh, P.M. (2019). Biomonomers for Green Polymers: Introduction. *Bio Monomers for Green Polymeric Composite Materials*, pp.1-24.

Wang, S.; Liu, W.; Yang, D.; Qiu, X. (2019). Highly resilient lignin- containing polyurethane foam. *Ind. Eng. Chem. Res. 58*, 496–504.

Ward, I. M. (1971). *Mechanical Properties of Solid Polymers*; Wiley Interscience: New York.

Winnacker, M.; Rieger, B. (2016). Biobased Polyamides: Recent Advances in Basic and Applied Research. *Macromol. Rapid Commun. 37*, 1391–1413,

Wróblewska-Krepsztul, J., Rydzkowski, T., Borowski, G., Szczypiński, M., Klepka, T. and Thakur, V.K. (2018). Recent progress in biodegradable polymers and nanocomposite-based packaging materials for sustainable environment. *International Journal of Polymer Analysis and Characterization*, *23*(4), pp.383-395.

Wu, M.; Zhang, Y.; Peng, Q.; Song, L.; Hu, Z.; Li, Z.; Wang, Z. (2018). Mechanically strong plant oil-derived thermoplastic polymers prepared via cellulose graft strategy. *Appl. Surf. Sci. 458*, 495–502.

Xia, Y.; Larock, R. C. (2010). Castor oil-based thermosets with varied crosslink densities prepared by ring-opening metathesis polymerization (ROMP). *Polymer 51*, 2508–2514,

Xie, T., Kao, W., Sun, L., Wang, J., Dai, G. and Li, Z.(2020). Preparation and characterization of self-matting waterborne polymer–An overview. *Progress in Organic Coatings*, *142*, p.105569.

Yang, D.-P.; Li, Z.; Liu, M.; Zhang, X.; Chen, Y.; Xue, H.; Ye, E.; Luque, R. (2019). Biomass-derived carbonaceous materials: recent progress in synthetic approaches, advantages, and applications. *ACS Sustainable Chem. Eng. 7*, 4564–4585.

Yan, Y., Sun, Y., Li, B. and Zhou, P. (2022). An experimental study of PMMA precision cryogenic micro-milling. *Biomaterials and Polymers Horizon*, *1*(1), pp.1-7.

Yuan, L.; Wang, Z.; Trenor, N. M.; Tang, C. (2015). Robust Amidation transformation of plant oils into fatty derivatives for sustainable monomers and polymers. *Macromolecules 48*, 1320–1328,

Zafar, R., Zia, K.M., Tabasum, S., Jabeen, F., Noreen, A. and Zuber, M. (2016). Polysaccharide based bionanocomposites, properties and applications: A review. *International journal of biological macromolecules*, *92*, pp.1012-1024.

Zafar, F.; Ghosal, A.; Sharmin, E.; Chaturvedi, R.; Nishat, N. (2019). A review on cleaner production of polymeric and nanocomposite coatings based on waterborne polyurethane dispersions from seed oils. *Prog. Org. Coat. 131*, 259–275.

Zakzeski, J., Bruijnincx, P.C., Jongerius, A.L. and Weckhuysen, B.M. (2010). The catalytic valorization of lignin for the production of renewable chemicals. *Chemical reviews*, *110*(6), pp.3552-3599.

Zhang, X.; Jeremic, D.; Kim, Y.; Street, J.; Shmulsky, R. (2018). Effects of Surface

Functionalization of Lignin on Synthesis and Properties of Rigid Bio-Based Polyurethanes Foams. *Polymers 10*, 706.

Zhang, C.; Wu, H.; Kessler, M. R. (2015). High bio-content polyurethane composites with urethane modified lignin as filler. *Polymer*, *69*, 52–57.

Zhang, C.; Garrison, T. F.; Madbouly, S. A.; Kessler, M. R. (2017). Recent advances in vegetable oil-based polymers and their composites. *Prog. Polym. Sci. 71*, 91–143.

Zhang, C.; Madbouly, S. A.; Kessler, M. R. (2015). Bio-based Polyurethanes Prepared from different vegetable oils. *ACS Appl. Mater. Interfaces 7*, 1226–1233.

Zhao, Y., Teixeira, J.S., Gänzle, M.M. and Saldaña, M.D. (2018). Development of antimicrobial films based on cassava starch, chitosan and gallic acid using subcritical water technology. *The Journal of Supercritical Fluids*, *137*, pp.101-110.

Zhou, X., Fang, C., Chen, J., Li, S., Li, Y. and Lei, W. (2016). Correlation of raw materials and waterborne polyurethane properties by sequence similarity analysis. *Journal of Materials Science & Technology*, *32*(7), pp.687-694.

Zhu, Y.; Romain, C.; Williams, C. K. (2016). Sustainable polymers from renewable resource. *Nature 540*, 354–362.